

SCIENTIFIC REPORTS



OPEN

Assessing Spatial and Temporal Patterns of Observed Ground-level Ozone in China

Wan-Nan Wang^{1,2}, Tian-Hai Cheng¹, Xing-Fa Gu¹, Hao Chen¹, Hong Guo¹, Ying Wang¹, Fang-Wen Bao^{1,2}, Shuai-Yi Shi^{1,2}, Bin-Ren Xu^{1,2}, Xin Zuo^{1,2}, Can Meng^{1,2} & Xiao-Chuan Zhang^{1,2}

Elevated ground-level ozone (O₃), which is an important aspect of air quality related to public health, has been causing increasing concern. This study investigated the spatiotemporal distribution of ground-level O₃ concentrations in China using a dataset from the Chinese national air quality monitoring network during 2013–2015. This research analyzed the diurnal, monthly and yearly variation of O₃ concentrations in both sparsely and densely populated regions. In particular, 6 major Chinese cities were selected to allow a discussion of variations in O₃ levels in detail, Beijing, Chengdu, Guangzhou, Lanzhou, Shanghai, and Urumchi, located on both sides of the Heihe-Tengchong line. Data showed that the nationwide 3-year MDA8 of ground-level O₃ was 80.26 μg/m³. Ground-level O₃ concentrations exhibited monthly variability peaking in summer and reaching the lowest levels in winter. The diurnal cycle reached a minimum in morning and peaked in the afternoon. Yearly average O₃ MDA8 concentrations in Beijing, Chengdu, Lanzhou, and Shanghai in 2015 increased 12%, 25%, 34%, 22%, respectively, when compared with those in 2013. Compared with World Health Organization O₃ guidelines, Beijing, Chengdu, Guangzhou, and Shanghai suffered O₃ pollution in excess of the 8-hour O₃ standard for more than 30% of the days in 2013 to 2015.

Ozone (O₃) at the ground level creates a major air pollutant that affects human health¹. High concentrations of ground-level O₃ can cause cardiovascular and respiratory dysfunction^{2–5}, and contribute to increased levels of mortality, especially for elderly people⁶. An increase of 21.3 μg/m³ in the mean 3-day running concentration of O₃ resulted in a 6.6% increase in daily deaths in the warm season caused by respiratory diseases (95% CI:1.8, 11.8)⁷ in Montreal, Quebec. In China, a 10 μg/m³ increase of the maximum 8-h average concentration of O₃, was reflected in increases in non-accidental mortality, cardiovascular mortality, and respiratory mortality by 0.42% (95% CI, 0.32–0.52), 0.44% (95% CI, 0.17–0.70), and 0.50% (95% CI, 0.22–0.77), respectively⁸. The World Health Organization (WHO) set a guideline of 100 μg/m³ for a maximum daily 8-hour average (MDA8) exposure to ground-level O₃. Keeping air pollution below this concentration will provide adequate protection for public health, although some health effects may occur below this level⁹. The Review of Evidence on Health Aspects of Air Pollution summarized newly accumulated scientific evidence related to the adverse effects of O₃ on human health at levels below the WHO guideline. Additionally, the Review of Evidence on Health Aspects of Air Pollution points out that O₃ is involved in the formation of secondary inorganic and organic particulate matter (PM) in the outdoor environment. In addition, it shows that the reaction of O₃ with common indoor volatile organic compounds (VOCs) generates a plethora of various compounds, many of which have been proposed to be respiratory irritants¹⁰.

Ground-level O₃ is mainly produced during chemical reactions when mixtures of organic precursors (CH₄ and non-methane volatile organic carbon, NMVOC), CO, and nitrogen oxides (NO_x = NO + NO₂) are exposed to the UV radiation in the troposphere¹¹. The most important interactions that drive the production of O₃ concentrations in the troposphere and some of the related feedback mechanisms have been discussed thoroughly^{12,13}.

In the last few decades, the burning of biomass has been recognized as an important source of O₃ precursors^{14–16}. Because terrestrial vegetation is the dominant source of atmospheric VOCs, vegetation can have a large effect on the distribution of O₃ and its precursors¹⁷. In 2008, China was recently determined to be the largest contributor to Asian emissions of CO, NO_x, NMVOC, and CH₄; the growth rates of these emissions from China were

¹State Key Laboratory of Remote Sensing Science, Institute of Remote Sensing and Digital Earth, Chinese Academy of Sciences, Beijing, 100101, China. ²University of Chinese Academy of Sciences, Beijing, 100101, China. Correspondence and requests for materials should be addressed to T.-H.C. (email: chength@radi.ac.cn)

also the largest in Asia because of the current continuous increase in energy consumption, economic activity, and infrastructural development¹⁸. A complex coupling of primary emissions, chemical transformation, and dynamic transport at different scales has created the O₃ problem¹⁹. In addition, the chemical transformation for O₃ has nonlinear chemistry with respect to its precursors and the contributions from both local and regional sources²⁰. The effect of VOCs and NO_x on O₃ formation can be described by VOC-limited or NO_x-limited regimes^{21–23}. At elevated NO_x levels, which is typical of the polluted urban environment, O₃ levels can be severely depleted locally because O₃ reacts directly with emitted NO in a reaction known as the ‘NO_x titration effect.’ The rate of the process of O₃ scavenging in the urban environment by titration with NO_x gradually declines as NO_x urban emissions are reduced when emissions are controlled. O₃ concentrations in urban areas have increased as emissions of NO have declined. This will have an important effect on control measures and will result in an increase in the exposure of urban populations to O₃ in the coming decade²⁴.

Because of the importance of O₃ as it relates to air quality and public health, O₃ has received continuous attention from both the scientific and regulatory communities²⁵. Numerous long-term monitoring sites have been established worldwide to observe the spatial and temporal features of ground-level O₃. The Air Quality System of the U.S. Environmental Protection Agency contains data related to ambient air pollution collected from thousands of monitors. Regions with large urban atmospheres with poor ventilation in the Americas, such as the Los Angeles, Mexico City and Santiago de Chile metropolitan areas, have experienced O₃ in excess of 400 µg/m³ for short-term ground-level O₃ concentrations²⁶. A trend analysis in Europe with the O₃-monitoring sites data covering the 12 years from 1993 to 2005 showed that some Mediterranean cities recorded 1-hour average ground-level O₃ concentrations exceeding 300 µg/m³²⁷. The satellite remote sensing is another widely used and provides useful way to investigate the ground-level distribution of O₃. The spatial coverage of the new generation of nadir-looking instruments onboard polar-orbiting satellites, such as the Global Ozone Monitoring Experiment, Infrared Atmospheric Sounding Interferometer and Ozone Monitoring Instrument, makes them interesting tools that can be used to monitor tropospheric O₃ over large regions, helping researchers to assess any problems related to air quality and transport^{28–31}. Nevertheless, differences still remain between a tropospheric column O₃ derived from satellite observation and ground monitor data^{32–34}.

Rapid industrialization and urbanization in China have led to high concentrations of ground-level O₃³⁵, which often cause concerns related to public health in this populous country. Although numerous studies have been conducted O₃ epidemiology^{36,37}, such studies are less commonly available in China^{38–43}. High O₃ concentrations exceeding the national ambient air quality standards have been frequently observed in large cities of China^{44–48}. Recent studies have also indicated increasing O₃ trends exist in several highly urbanized regions of China^{49,50}. Meanwhile, few types of research have focused on the nationwide spatial and temporal variability of ground-level O₃ concentrations in China. The Chinese government at various levels began to establish a national air quality monitoring network in 2012, which released real-time ground-level O₃ monitoring data to the public. With the establishment of a national air quality monitoring network, large-scale real-time ground-level O₃ monitoring data become available.

The spatial and temporal variability of ground-level O₃ concentrations in China has been studied using a dataset from the national air quality monitoring network covering 2013–2015. The present paper investigates and demonstrates the spatial and temporal distribution of ground-level O₃ on a nationwide scale, including its yearly, monthly and diurnally patterns of ground-level O₃ concentration. In order to provide further insight into the variations between densely and sparsely populated regions, 6 major cities lied on both sides of Heihe-Tengchong line were selected to discuss in detail: Beijing, Chengdu, Guangzhou, Lanzhou, Shanghai, and Urumchi, their locations showed in Fig. 1.

Results

Spatial distribution of ground-level O₃. Figure 1 shows spatial distribution of 3-year MDA8 ground-level O₃ concentrations during 2013–2015. A total of 717 stations with fixed locations and continuous operation were selected through 2013–2015. The 3-year averaged ground-level O₃ concentration was 80.26 µg/m³. Specifically, the 3-year averaged ground-level O₃ concentrations were 81.21 µg/m³ and 74.35 µg/m³ in the densely (617 stations) and sparsely (100 stations) populated regions, respectively. Obviously, the large number of stations in the densely populated area biased the national data in favor of a larger number. The spatial distribution of averaged ground-level ozone MDA8 concentrations from 2013 to 2015 was displayed in supplemental material.

The 3-year averaged O₃ concentrations of the densely and sparsely populated regions were analyzed as independent samples in a T-test using IBM SPSS Statistics (Table 1). The T-test for equality of means showed that the O₃ level and variations between the densely and sparsely populated region were significantly different (Sig. < 0.001 with α = 0.05).

Note that a strong positive correlation between exists between surface O₃ level and elevation^{51–53}, causing the concentrations of O₃ to often exceed recommended levels at stations located on the Qinghai-Tibet Plateau. To better visualize the situation in the densely populated region of eastern China, we used the Beijing-Tianjin-Hebei (BTH) metropolitan area along with the Yangtze River Delta (YRD) and the Pearl River Delta (PRD) regions for examples. These represent the most highly developed and populated regions in China. The 3-year mean ground-level O₃ concentrations of BTH, YRD, and PRD were 82.14, 89.59, and 86.34 µg/m³, respectively.

Temporal distribution of ground-level O₃. Figure 2 shows mean monthly 3-year O₃ MDA8 concentrations during 2013–2015. Generally, the monthly variability of ground-level O₃ concentrations peaked in summer and were the lowest in winter. The peak and valley values of monthly ground-level O₃ concentrations in the densely populated regions were 107.38 µg/m³ and 46.97 µg/m³, which were reached in August and December, respectively. In the sparsely populated region, peak and valley values were 112.15 µg/m³ and 40.18 µg/m³, and were reached in July and December, respectively.

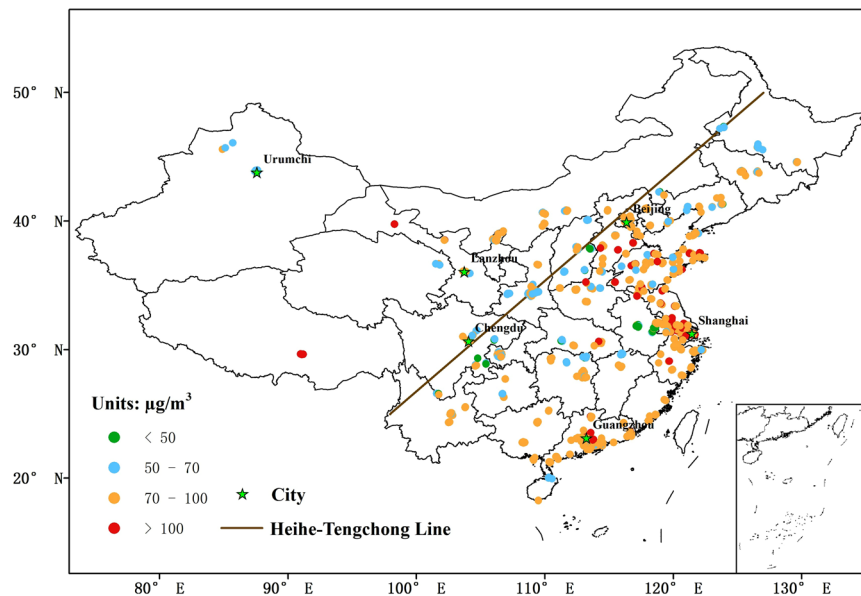


Figure 1. The spatial distribution of three-year averaged ground-level MDA8 ozone concentrations ($\mu\text{g}/\text{m}^3$) during 2013–2015 and the location of 6 cities in China. We selected the same monitoring stations from 2013 to 2015, and calculated each station’s 3-year averaged ground-level ozone maximum daily 8-hour average (MDA8). This data was then imported into ArcGIS software (ArcGIS Desktop version 10.0, ESRI, Redlands, CA, USA; URL, <http://www.esri.com>); different concentration levels were displayed using various colors.

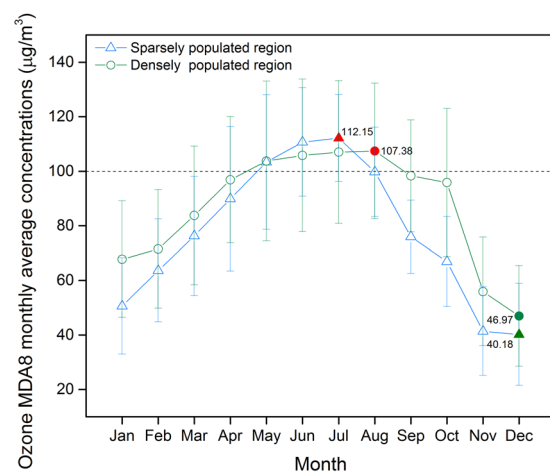


Figure 2. Monthly distribution of three-year averaged ground-level maximum daily 8-hour average (MDA8) ozone concentrations during 2013–2015.

<i>t</i>	<i>df</i>	Sig. (2-tailed)	Mean Difference	Sta. Error Difference	95% Confidence interval of the Difference	
					Lower	Upper
−4.03	715	0.00063	−6.86	1.70	−10.2	−3.51

Table 1. Variations in T-test results for independent samples of the three-year averaged ozone concentrations between the densely and sparsely regions. Note: *t* is the computed T-test statistic, *df* is the degrees of freedom, Sig. (2-tailed) is the *p*-value corresponding to the given test statistic and degrees of freedom, Mean Difference is the difference between the sample mean, Std. Error Difference is the different in the standard error.

Figure 3 shows hourly 3-year average O_3 concentrations during 2013–2015. Ground-level O_3 concentrations showed a typical diurnal cycle with a minimum in the morning and a maximum in the afternoon. In the densely populated region, the maximum and minimum values of 3-year hourly averaged ground-level O_3 concentrations

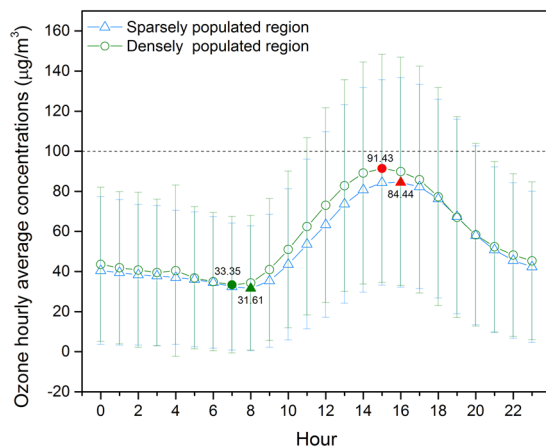


Figure 3. Hourly distribution of three-year averaged ground-level ozone concentrations during 2013–2015.

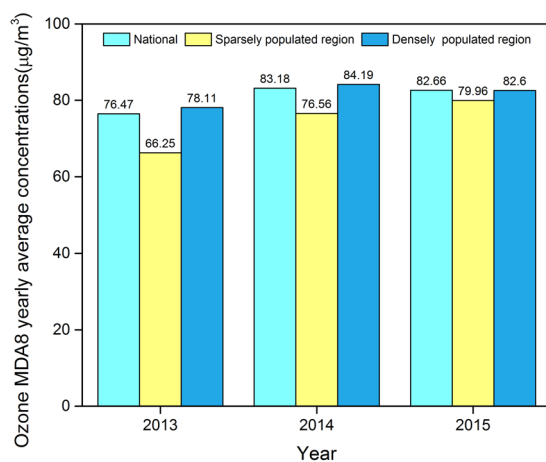


Figure 4. The maximum daily eight-hour average (MDA8) concentrations of annual averaged ground-level ozone in 2013–2015.

were 91.43 and 33.35 $\mu\text{g}/\text{m}^3$, and were observed at 15:00 and 7:00, respectively. In the sparsely populated region, the maximum and minimum values were 84.44 and 31.67 $\mu\text{g}/\text{m}^3$, observed at 16:00 and 8:00, respectively.

The hourly mean concentrations of ground-level O_3 in the densely populated region were higher than those measured in the sparsely populated region. In addition, a small peak existed at 4:00 for diurnal concentrations in the densely populated region, which was not found in the sparsely populated region; this can perhaps be explained by the accumulation of O_3 precursors because of the relatively low boundary layer in this region⁴⁶.

The annual variety of ground-level O_3 concentrations. In the past 3 years, the national highest annual mean of the yearly ground-level O_3 MDA8 concentrations from 2013 to 2015 was 83.18 $\mu\text{g}/\text{m}^3$ in 2014, which was up by 9% when compared with 2013 (Fig. 4). For 2015, this figure was 82.66 $\mu\text{g}/\text{m}^3$, and had remained at approximately the same level as was observed in 2014. In the densely populated region, the highest annual average concentration in the past 3 years appeared in 2014. In the sparsely populated region, the annual average concentrations of ground-level O_3 increased year by year from 2013 to 2015.

Ground-level O_3 is subject to *in situ* chemical reactions and physical processes that are directly affected by precursor emissions, solar radiation and other meteorological factors⁵⁴. NO_x and VOCs play important roles in O_3 formation, while NO and VOCs concentrations were not included in the data collected by the national air quality monitoring network. Therefore, yearly NO_2 concentrations variations were measured from 2013 to 2015.

The yearly averaged NO_2 concentrations decreased year by year from 2013 to 2015 (Fig. 5). The national NO_2 mean was 31.1 $\mu\text{g}/\text{m}^3$ in 2015, and had declined by nearly 30% when compared with 2013. The Chinese State Council released the 'Atmospheric Pollution Prevention and Control Action Plan' on September 2013, in which they decided to implement critical strategies designed to control the burning of coal and vehicle exhaust, as well as for the management of power plants and so on⁵⁵. After a 2-year effort, as one of the O_3 precursors, the NO_2 concentrations have indeed decreased since 2013⁵⁶. In contrast, the national yearly average O_3 concentration in 2015 was higher than that in 2013, and the increase in the ground-level O_3 concentrations in the sparsely populated region was greater than that in the densely populated region.

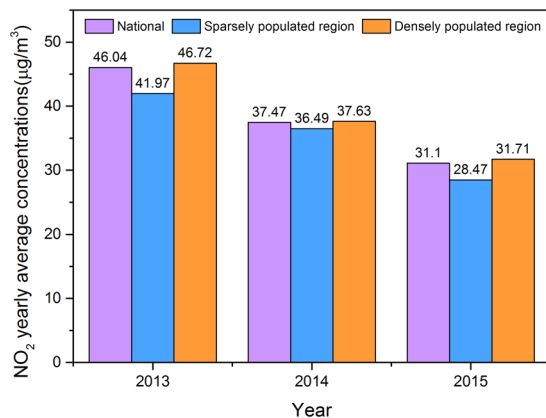


Figure 5. The annual averaged NO₂ concentrations of 2013–2015.

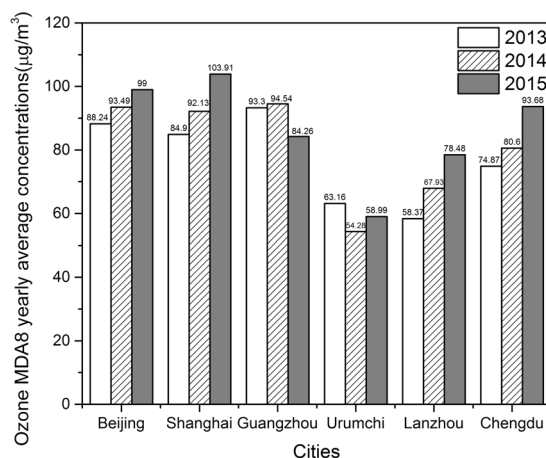


Figure 6. The maximum daily eight-hour average (MDA8) concentrations of annual averaged ground-level ozone in 6 cities during 2013–2015.

The levels of O₃ and NO₂ are inextricably linked because of the chemical coupling of O₃ and NO_x. Therefore, the response to reduction in the emission of NO_x is remarkably non-linear⁵⁷ and any resultant reduction in the level of NO₂ is invariably accompanied by an increase in the level of O₃⁵⁸. While ground-level O₃ formation comes from a complex coupling of primary emissions and chemical transformation, increasing the ground-level O₃ could not only be caused by the decline in NO₂ in China. Ma, *et al.*⁵⁴ reported that the change of VOCs emissions might have played a more important role in the O₃ increase than the effect of NO_x in the northern part of eastern China⁵⁴. Observations have shown that Beijing's efforts to control air pollution were somehow effective in cutting O₃ precursors, but still left a relatively high amount of ground-level O₃; researchers surmised that this resulted from potential contributions from VOCs and regional transport near Beijing⁵⁹. Analysis using a smog production algorithm proved that the reduction in VOC is generally useful in reducing the photochemical production of O₃ while the combined reduction of NO_x and VOC would be important to efforts to reduce the appearance of O₃ episodes in the PRD⁶⁰. The computation of the production rate of total oxidants (O₃ + NO₂) indicated that the trends of ambient oxidant levels largely depended on the ratio of VOCs/NO_x⁶¹, and that a more rapid reduction in VOC reactivity would be very effective for decreasing total oxidants⁵⁹.

Figure 6 shows the yearly mean MDA8 O₃ concentrations from 2013 to 2015 in 6 cities. Generally, yearly mean O₃ concentrations in Beijing, Chengdu, Guangzhou, and Shanghai remained a relative high when compared with those of Lanzhou and Urumchi. Yearly average O₃ MDA8 concentrations in Beijing, Chengdu, Lanzhou, and Shanghai in 2015 increased 12%, 25%, 34%, 22%, respectively, when compared with those in 2013. Interestingly, yearly O₃ concentrations in 2015 decreased nearly 11% when compared with those in 2014 in Guangzhou. Except for reducing NO_x and CO emissions, this change also might have been caused by a pilot project launched in Guangzhou to take the lead in controlling VOC emissions that started in 2012.

Figure 7 shows ground-level O₃ MDA8 monthly concentrations from 2013 to 2015 in the densely populated region. The peak mean values occurred in August for 2013, June for 2014, May for 2015. The monthly mean concentration exceeded 100 µg/m³ during 2, 4, and 3 in 2013, 2014, and 2015, respectively, with peak monthly mean values 101.96, 111.24, and 105.68 µg/m³, respectively. The lowest monthly mean MDA8 values of the 3 years all occurred during December, with the values declining every year (50.49, 47.00, and 44.57 µg/m³ for 2013, 2014, and 2015, respectively).

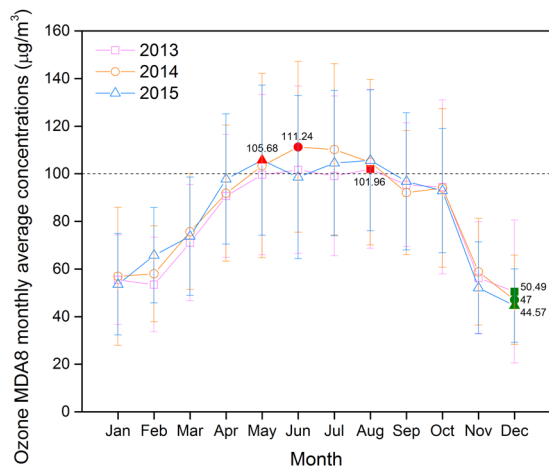


Figure 7. Monthly distribution of the maximum daily eight-hour average (MDA8) concentrations of ground-level ozone in densely populated regions of China during 2013–2015.

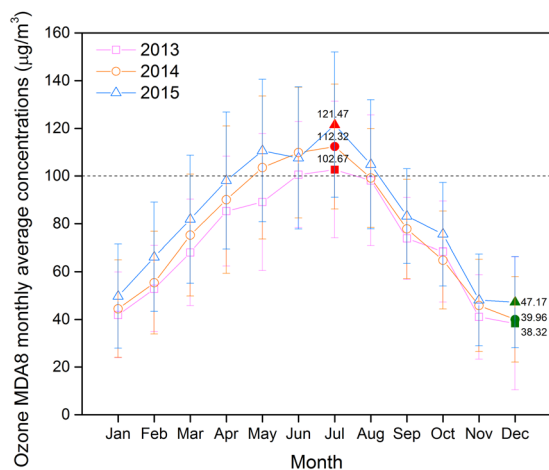


Figure 8. Monthly distribution of the maximum daily eight-hour average (MDA8) concentrations of ground-level ozone in sparsely populated region during 2013–2015.

Figure 8 shows the monthly ground-level MDA8 O_3 concentrations from 2013 to 2015 in the sparsely populated region. The monthly mean peak and valley values of the 3 years in this region all occurred in July and December, respectively. In addition, the number of months with the monthly mean concentration above $100 \mu\text{g}/\text{m}^3$ increased from 2 to 3 to 4 months in 2013, 2014, and 2015, respectively.

Figure 9 shows the monthly mean MDA8 O_3 concentrations from 2013 to 2015 in 6 cities. In Beijing, O_3 concentrations remained relatively high from April to September, with lower concentrations in the winter months. O_3 concentrations varied widely in Beijing from 2013 to 2014. The mean concentrations even peaked above $150 \mu\text{g}/\text{m}^3$ in August 2014 and June 2015, while the fell below $40 \mu\text{g}/\text{m}^3$ in December and January. In Shanghai, high O_3 concentrations were observed from almost all of April to most of October, a little longer than occurred in Beijing. Shanghai lies in southern China and near the sea where the meteorological conditions remain suitable for O_3 formation in October. The monthly mean concentration remained above $100 \mu\text{g}/\text{m}^3$ from June to August (3 months) in 2013 and from April to October in 2014 (7 months), and from March to October (8 months) in 2015. In Guangzhou, high O_3 concentrations were observed from June to October, starting later than in Beijing and Shanghai. The highest mean O_3 concentrations of 2013 and 2014 all occurred in October. This may have occurred because Guangzhou is located at a lower latitude and experiences a subtropical monsoon climate. Here, more sunlight and higher temperatures could favor greater O_3 formation in summer, while typhoon rainstorms were also frequent in summer, which brought in clean ocean air that diluted the high O_3 levels. The occurrence of fewer typhoon-related rainstorms and suitable meteorological conditions for O_3 formation led to an increase in ground-level O_3 concentrations in October.

In Urumchi, O_3 concentrations remained relatively low when compared with the other 5 cities. Relatively high monthly O_3 concentrations were observed from June to August. In November and December, the mean O_3 concentrations can fall below $20 \mu\text{g}/\text{m}^3$. Urumchi is located in northwestern China at a comparatively high



Figure 9. Monthly distribution of the maximum daily eight-hour average (MDA8) concentrations of ground-level ozone in six cities during 2013–2015.

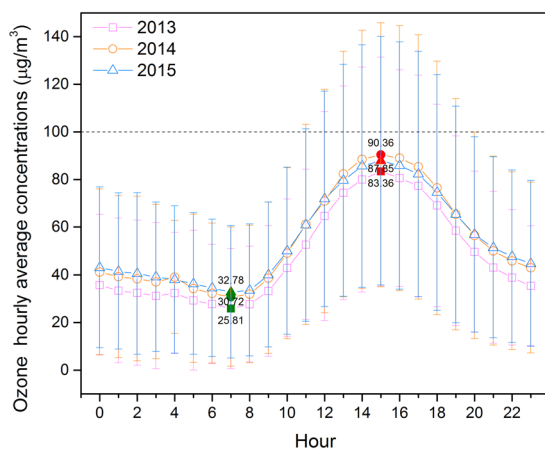


Figure 10. Hourly distribution of the maximum daily eight-hour average (MDA8) concentrations of ground-level ozone in densely populated regions during 2013–2015.

average elevation of 800 m. This city has stronger sunlight and less rainfall in summer than most of China, while its longer winter and lower temperatures inhibited O_3 formation to some degree. In Lanzhou, the months of relatively high O_3 concentrations appeared in April to August. Although O_3 monthly mean concentrations remained below $100 \mu\text{g}/\text{m}^3$, the monthly and yearly mean O_3 concentrations increased year by year from 2013 to 2015. In Chengdu, the O_3 concentrations remained at a high level from April to August, even reaching nearly $160 \mu\text{g}/\text{m}^3$ in May and July 2015. Chengdu lies in the western Sichuan Basin where the western mountains often block the airflow. Affected by the basin effect, this region has poor gas diffusion capacity and high temperatures in summer. Therefore, the O_3 accumulation easily reach a high level in summer in Chengdu.

Figure 10 shows the hourly ground-level O_3 concentrations from 2013 to 2015 in the densely populated region. The timing of the peak and valley values of the hourly mean concentrations of all 3 years did not change significantly in the densely populated region. These peak values were all reached at 15:00 and were 83.36, 90.36,

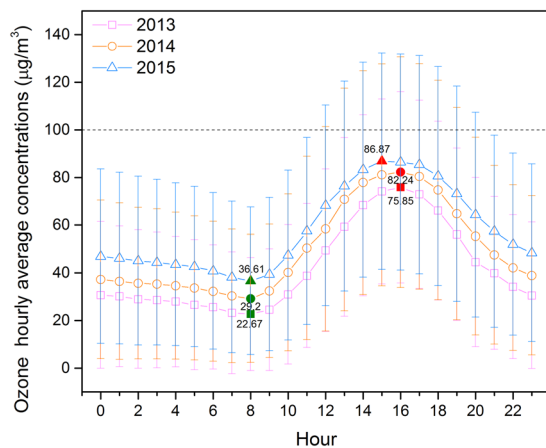


Figure 11. Hourly distribution of the maximum daily eight-hour average (MDA8) concentrations of ground-level ozone concentrations in sparsely populated regions during 2013–2015.

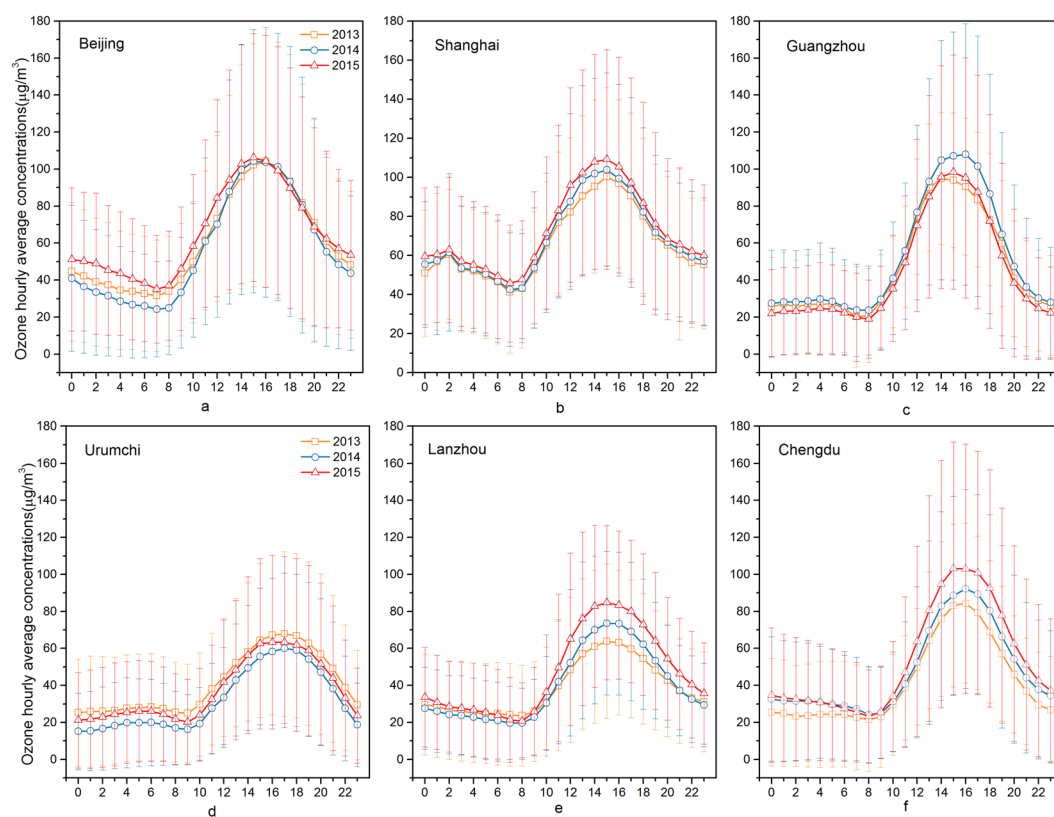


Figure 12. Hourly distribution of the maximum daily eight-hour average (MDA8) concentrations of ground-level ozone concentrations in six cities during 2013–2015.

and $87.85 \mu\text{g}/\text{m}^3$ for 2013, 2014, and 2015, respectively. Corresponding, the lowest values were all reached at 07:00 and were 25.81 , 30.72 , and $32.78 \mu\text{g}/\text{m}^3$ for 2013, 2014, and 2015, respectively. In the densely populated region, a smaller peak occurred at 4:00 and was not observed in the sparsely populated region.

Figure 11 shows the hourly ground-level O_3 hourly concentrations from 2013 to 2015 in the sparsely populated region. The peak values were 75.85 , 82.24 , and $86.87 \mu\text{g}/\text{m}^3$ for 2013, 2014, 2015, respectively. The valleys were 22.67 , 29.2 , and $36.61 \mu\text{g}/\text{m}^3$ for 2013, 2014, 2015, respectively. The timing of the peak values of 2015 at 15:00 were advanced by 1 hour when compared with those of 2013 and 2014 at 16:00, while timing of the valley values were consistent of 3 years at 8:00 in sparsely populated region.

Figure 12 shows the hourly mean O_3 concentrations from 2013 to 2015 in 6 cities. As a typical product of photochemical reactions, the ground-level O_3 concentrations was closely related to the intensity of solar radiation. The production of O_3 began after sunrise and it accumulated until reaching peak concentrations in the

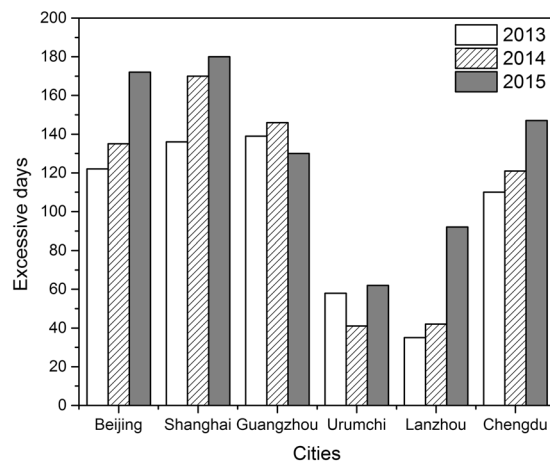


Figure 13. The number of days of exceeding the maximum daily eight-hour average (MDA8) concentrations of ground-level ozone in six cities during 2013–2015.

afternoon. With sunset, the photochemical reactions declined rapidly to near zero without solar radiation, so that O_3 reduction reactions occurred because of NO_x , CO, NMHC and other O_3 precursors, resulting in low levels of O_3 concentrations in the night.

In Beijing, Guangzhou, and Shanghai ground-level O_3 concentrations started to increase at almost exactly 7:00, and peaked at about 15:00. In Lanzhou and Chengdu, it began to increase at 8:00 and reached peak concentrations at around 16:00. In Urumchi, the latitude and time difference caused O_3 concentrations to begin to increase at 9:00 and they reached peak values at 17:00. Note that all of China uses a single time zone, but spans 5 time zones of other countries, which is part of the cause of this difference.

Figure 13 shows MDA8 for O_3 exceeded the standard on some days from 2013 to 2015 in 6 cities. In Beijing, Chengdu, Lanzhou, and Shanghai, the number of days exceeding the standard when compared with the WHO O_3 guideline (MDA8 O_3 above $100\mu g/m^3$) increased year by year from 2013 to 2015. Beijing, Chengdu, Guangzhou, and Shanghai experienced O_3 pollution with concentrations in excess of the 8-hour standard for more than 30% of the year from 2013 to 2015. Beijing and Shanghai even suffered O_3 pollution with concentrations in excess of the 8-hour standard for more than 45% in 2015. Corresponding to the decrease in O_3 yearly concentration, the number of days when the standard was exceeded also declined in 2015 in Guangzhou.

Discussion

The results from the present analysis could improve our understanding of ground-level O_3 at a fine spatiotemporal resolution in China, given the lack of historic long-term monitoring.

The nationwide and regional three-year ground-level MDA8 O_3 concentrations were provided above. Ground-level O_3 concentrations showed a monthly variability peaking in summer and reaching their lowest in winter, while the diurnal cycle exhibited a minimum in the morning and peaked in the afternoon. Unlike the decrease in NO_2 concentrations from 2013, the O_3 concentrations began to increase after the implementation of critical emission control strategies in China. Climate, geographical location and anthropogenic emissions of precursors have caused the monthly O_3 concentrations in different cities to vary widely. Compared with WHO O_3 guideline, Beijing, Chengdu, Guangzhou, and Shanghai suffered O_3 pollution in excess of the 8-hour O_3 standard for more than 30% of the days in 2013 to 2015.

The fact that O_3 concentrations varied on a nationwide scale and in 6 major cities after the implementation of critical air control strategies can provide decision support to future policy formulation in China. The Chinese State Council released the ‘Atmospheric Pollution Prevention and Control Action Plan’ on September 2013. Critical emission control strategies have been carried out that are designed to reduce the concentrations of particular matter smaller than $2.5\mu m$ ($PM_{2.5}$) and other pollutant gases. An urgent need exists for researchers to evaluate the effects of these air quality control strategies on variations in the concentration of ground-level O_3 . For 2015, report of the Chinese Ministry for Environmental Protection in 2016 showed that concentrations of $PM_{2.5}$ decreased generally in China⁵⁷. The present study shows that the O_3 problem has become increasingly prominent in China. The national yearly average O_3 concentration in 2015 was higher than that in 2013, and the increase of ground-level O_3 concentrations in the sparsely populated region was greater than that in the densely populated region. The yearly average MDA8 O_3 concentrations in Beijing, Chengdu, Lanzhou, and Shanghai in 2015 increased by 12% to 34%, respectively, compared with that in 2013. Beijing and Shanghai even suffered O_3 pollution with concentrations in excess of the 8-hour standard for more than 45% of all days in 2015. With large numbers of people affected, the dramatic threat of O_3 to public health and its wide range of influence cannot be ignored in China.

With our understanding that the complexity of the air pollution mixture in China has improved, the need for specific strategies designed to limit and control air pollution for individual pollutants has become increasingly apparent. VOCs and NO_x all play important roles in the formation of O_3 at ground-level, and their effect on O_3 is nonlinear. As a result, simply reducing levels of NO_x may be ineffective in managing the O_3 problem. This, however, risks further increases in O_3 because a VOCs/ NO_x ratio more favorable to O_3 production may be

reached. Few long-term and nationwide observational data are available for VOCs, which only serves to limit our understanding of O₃ production and control. It is time for the Chinese government to begin monitoring VOCs and to conduct related environmental monitoring. More specifics related to the relationships between various types of atmospheric pollution should be studied and considered during the formulation of revised management strategies.

Methods

O₃ monitoring data. The Department of the Environment continuously operates and maintains the national air quality monitoring network of China, an effort that began in 2012. At each monitoring site, the concentration of O₃ was measured using the ultraviolet absorption spectrometry method and differential optical absorption spectroscopy. The instrumental operation, maintenance, data assurance and quality control were properly conducted based on the most recent revisions of China Environmental Protection Standards⁶². The network was comprised of nearly 950 monitoring stations in 2013, which was extended to approximately 1500 stations by the end of 2015. The present study employed data from Jan. 2013 to Dec. 2015.

Maximum daily 8-hour average O₃. When considering the affects associated with controlled O₃ exposures on health outcomes^{63–66}, WHO set a guideline value for O₃ exposure of 100 µg/m³ for a maximum period of 8 hours per day⁹. Therefore, we calculated an MDA8 for O₃ concentration of each station. MDA8 O₃ concentrations were calculated using greater than 5 hourly averages that were available (not zero) every 8 hours. Generally, if fewer than 6 hours of O₃ concentration data were available for a certain 8-hour period, then this 8-hour average was assigned as the 'missing' value⁶⁷. In the present study, the 'missing' values (zero) was not considered in the next analysis. Finally, the maximum value of the daily 8-hour averages were used as the valid MDA8.

Delimitation of population aggregation. Heihe-Tengchong line serves as the delimitation line of population aggregation in China. The densely and sparsely populated regions were southeast and northwest of the line, respectively. About 94% of China's population lives in 43% of the land area, creating this pattern of dense and sparse populations southeast (325.84 people/km²) and northwest (14.68 people/km²) of the line, respectively, and this pattern is not expected to fundamentally change for a relatively long time⁶⁸.

Average calculation. A total of 717 stations with fixed locations and continuous operation having valid MDA8 O₃ values were selected through 2013–2015. Among the 717 stations through these 3 years, 617 and 100 stations were located in the densely and sparsely populated regions, respectively. The monthly and annual average concentrations of ground-level O₃ were the means of the available MDA8 data from all monitoring sites in a specific area. Diurnally average concentrations were calculated using each hourly concentration of all sites. Statistical analyses were carried out using Microsoft Excel 2010 and IBM SPSS Statistics 22.

References

- Anenberg, S. C. *et al.* Intercontinental Impacts of Ozone Pollution on Human Mortality. *Environ Sci Technol* **43**, 6482–6487 (2009).
- West, J. J., Fiore, A. M., Horowitz, L. W. & Mauzerall, D. L. Global health benefits of mitigating ozone pollution with methane emission controls. *P Natl Acad Sci USA* **103**, 3988–3993 (2006).
- Jerrett, M. *et al.* Long-Term Ozone Exposure and Mortality. *New Engl J Med* **360**, 1085–1095 (2009).
- Guo, Y. M. *et al.* The association between air pollution and mortality in Thailand. *Sci Rep-Uk* **4** (2014).
- Yang, W. S., Wang, X., Deng, Q., Fan, W. Y. & Wang, W. Y. An evidence-based appraisal of global association between air pollution and risk of stroke. *Int J Cardiol* **175**, 307–313 (2014).
- Levy, J. I., Chemerynski, S. M. & Sarnat, J. A. Ozone exposure and mortality - An empiric Bayes metaregression analysis. *Epidemiology* **16**, 458–468 (2005).
- Goldberg, M. S. *et al.* Associations between daily cause-specific mortality and concentrations of ground-level ozone in Montreal, Quebec. *Am J Epidemiol* **154**, 817–826 (2001).
- Yan, M. L., Liu, Z. R., Liu, X. T., Duan, H. Y. & Li, T. T. Meta-analysis of the Chinese studies of the association between ambient ozone and mortality. *Chemosphere* **93**, 899–905 (2013).
- WHO. *Air Quality Guidelines: Global Update 2005: Particulate Matter, Ozone, Nitrogen Dioxide and Sulfur Dioxide* (World Health Organization, 2006).
- WHO. Regional Office for Europe. *Review of evidence on health aspects of air pollution—REVIHAAP project: technical report.* Available at http://www.euro.who.int/__data/assets/pdf_file/0004/193108/REVIHAAP-Final-technical-report.pdf (Accessed: 16th January 2017).
- Simpson, D., Arneth, A., Mills, G., Solberg, S. & Uddling, J. Ozone - the persistent menace: interactions with the N cycle and climate change. *Curr Opin Env Sust* **9–10**, 9–19 (2014).
- Monks, P. S. *et al.* Tropospheric ozone and its precursors from the urban to the global scale from air quality to short-lived climate forcer. *Atmos Chem Phys* **15**, 8889–8973 (2015).
- U.S. EPA. *Assessment of the impacts of global change on regional U.S. air quality: a synthesis of climate change impacts on ground-level ozone* (National Center for Environmental Assessment Washington DC, 2009).
- Hao, W. M. & Liu, M. H. Spatial and temporal distribution of tropical biomass burning. *Global Biogeochem Cy* **8**, 495–503 (1994).
- Schultz, M. G. *et al.* Global Emissions from Wildland Fires from 1960 to 2000. *Global Biogeochem Cy* **22** (2008).
- Turquet, S. *et al.* Inventory of boreal fire emissions for North America in 2004: the importance of peat burning and pyro-convective injection. *J Geophys Res* **112** (2007).
- Guenther, A. *et al.* A global model of natural volatile organic compound emissions. *J Geophys Res* **100**, 8873–8892 (1995).
- Kurokawa, J. *et al.* Emissions of air pollutants and greenhouse gases over Asian regions during 2000–2008: Regional Emission inventory in Asia (REAS) version 2. *Atmos Chem Phys* **13**, 11019–11058 (2013).
- Jacob, D. J. *Introduction to Atmospheric Chemistry* (Princeton University Press, 1999).
- Xue, L. K. *et al.* Ground-level ozone in four Chinese cities: precursors, regional transport and heterogeneous processes. *Atmos Chem Phys* **14**, 13175–13188 (2014).
- Zhang, R. Y. *et al.* Industrial emissions cause extreme urban ozone diurnal variability. *Proc Natl Acad Sci. USA* **101**, 6346–6350 (2004).
- Tie, X. X. *et al.* Characterizations of chemical oxidants in Mexico City: A regional chemical dynamical model (WRF-Chem) study. *Atmos Environ* **41**, 1989–2008 (2007).

23. Geng, F. H. *et al.* Characterizations of ozone, NO_x, and VOCs measured in Shanghai, China. *Atmos Environ* **42**, 6873–6883 (2008).
24. Fowler, D. *et al.* Ground-level ozone in the 21st century: future trends, impacts and policy implications. *Roy Soc. Science Policy Rep* **15** (2008).
25. Wang, T. *et al.* Ozone pollution in China: A review of concentrations, meteorological influences, chemical precursors, and effects. *Sci Total Environ* **575**, 1582–1596 (2017).
26. U.S. EPA. *Peak air quality statistics for the six principal pollutants by metropolitan statistical area* (Environmental Protection Agency, 2003).
27. Fiala, J. *et al.* Air pollution by ozone in Europe in summer 2003. *Overview of exceedances of EC ozone threshold values during the summer season April–August 2003 and comparisons with previous years* (Copenhagen, European Environment Agency, 2003).
28. Dufour, G., Eremente, M., Orphal, J. & Flaud, J. M. IASI observations of seasonal and day-to-day variations of tropospheric ozone over three highly populated areas of China: Beijing, Shanghai, and Hong Kong. *Atmos Chem Phys* **10**, 3787–3801 (2010).
29. Jones, D. B. A. *et al.* Estimating the summertime tropospheric ozone distribution over North America through assimilation of observations from the Tropospheric Emission Spectrometer. *J Geophys Res* **113**, D18307 (2008).
30. Liu, X. *et al.* First directly retrieved global distribution of tropospheric column ozone from GOME: Comparison with the GEOS-CHEM model. *J Geophys Res-Atmos* **111** (2006).
31. Safieddine, S. *et al.* Summertime tropospheric ozone assessment over the Mediterranean region using the thermal infrared IASI/ MetOp sounder and the WRF-Chem model. *Atmos Chem Phys* **14**, 10119–10131 (2014).
32. Ziemke, J. R. *et al.* A global climatology of tropospheric and stratospheric ozone derived from Aura OMI and MLS measurements. *Atmos Chem Phys* **11**, 9237–9251 (2011).
33. Osterman, G. B. *et al.* Validation of Tropospheric Emission Spectrometer (TES) measurements of the total, stratospheric, and tropospheric column abundance of ozone. *J Geophys Res* **113**, D15S16 (2008).
34. Liu, X. *et al.* Ozone profile and tropospheric ozone retrievals from the Global Ozone Monitoring Experiment: Algorithm description and validation. *J Geophys Res* **110**, D20307 (2005).
35. Chinese Ministry of Environmental Protection (MEP), *China Environment Report of 2015*. Available at http://www.zhb.gov.cn/gkml/hbb/qt/201602/t20160204_329886.htm (Accessed: 10th August 2016).
36. Bell, M. L. *et al.* Climate change, ambient ozone, and health in 50 US cities. *Climatic Change* **82**, 61–76 (2007).
37. Bell, M. L., McDermott, A., Zeger, S. L., Samet, J. M. & Dominici, F. Ozone and short-term mortality in 95 US urban communities, 1987–2000. *JAMA* **292**, 2372–2378 (2004).
38. Yang, C. X. *et al.* Alternative ozone metrics and daily mortality in Suzhou: The China Air Pollution and Health Effects Study (CAPES). *Sci Total Environ* **426**, 83–89 (2012).
39. Li, T. *et al.* Short-term effects of multiple ozone metrics on daily mortality in a megacity of China. *Environ Sci Pollut Res* **22**, 8738–8746 (2015).
40. Tao, Y. B. *et al.* Estimated Acute Effects of Ambient Ozone and Nitrogen Dioxide on Mortality in the Pearl River Delta of Southern China. *Environ Health Persp* **120**, 393–398 (2012).
41. Wong, T. W. *et al.* Association between air pollution and general practitioner visits for respiratory diseases in Hong Kong. *Thorax* **61**, 585–591 (2006).
42. Liu, T. *et al.* The short-term effect of ambient ozone on mortality is modified by temperature in Guangzhou, China. *Atmos Environ* **76**, 59–67 (2013).
43. Zhang, Y. H. *et al.* Ozone and daily mortality in Shanghai, China. *Environ Health Persp* **114**, 1227–1232 (2006).
44. Wang, T., Ding, A. J., Gao, J. & Wu, W. S. Strong ozone production in urban plumes from Beijing, China. *Geophys Res Lett* **33** (2006).
45. Wang, T. *et al.* Air quality during the 2008 Beijing Olympics: secondary pollutants and regional impact. *Atmos Chem Phys* **10**, 7603–7615 (2010).
46. Zhang, J. *et al.* Ozone production and hydrocarbon reactivity in Hong Kong, Southern China. *Atmos Chem Phys* **7**, 557–573 (2007).
47. Zhang, Y. H. *et al.* Regional ozone pollution and observation-based approach for analyzing ozone-precursor relationship during the PRIDE-PRD2004 campaign. *Atmos Environ* **42**, 6203–6218 (2008).
48. Ran, L. *et al.* Ozone photochemical production in urban Shanghai, China: Analysis based on ground level observations. *J Geophys Res-Atmos* **114**, D1530110 (2009).
49. Xu, X. *et al.* Long-term trend of surface ozone at a regional background station in eastern China 1991–2006: enhanced variability. *Atmos Chem Phys* **8**, 2595–2607 (2008).
50. Wang, T. *et al.* Increasing surface ozone concentrations in the background atmosphere of Southern China, 1994–2007. *Atmos Chem Phys* **9**, 6217–6227 (2009).
51. Puxbaum, H., Gabler, K., Smidt, S. & Glatte, F. A One-Year Record of Ozone Profiles in an Alpine Valley (Zillertal Tyrol, Austria, 600–2000 M). *Atmos Environ a-Gen* **25**, 1759–1765 (1991).
52. Sandroni, S. & Bacci, P. Surface ozone in the prealpine and alpine regions. *Total Environ* **156**, 169–182 (1994).
53. Wunderli, S. & Gehrig, R. Influence of temperature of formation and stability of surface PAN and ozone. A two year field study in Switzerland. *Atmos Environ A. General Topics* **25**, 1599–1608 (1991).
54. Ma, Z. *et al.* Significant increase of surface ozone at a rural site, north of eastern China. *Atmos Chem Phys* **16**, 3969–3977 (2016).
55. Chinese State Council. *Atmospheric Pollution Prevention and Control Action Plan*, Available at http://www.gov.cn/zhengce/content/2013-09/13/content_4561.htm (Accessed: 15 August 2016).
56. Chinese Ministry of Environmental Protection (MEP), *'Atmospheric Pollution Prevention and Control Action Plan' mid-term evaluation report*, Available at http://www.zhb.gov.cn/xxgk/hjyw/201607/t20160706_357205.shtml (Accessed: 15 August 2016).
57. Fowler, D. *et al.* *Ozone in the United Kingdom - Fourth Report of the Photochemical Oxidants Review Group* (London, Institute of Terrestrial Ecology, 1997).
58. Han, S. *et al.* Analysis of the Relationship between O₃, NO and NO₂ in Tianjin, China. *Aerosol Air Qual Res* **11**, 128–139 (2011).
59. Zhang, Q. *et al.* Variations of ground-level O₃ and its precursors in Beijing in summertime between 2005 and 2011. *Atmos Chem Phys* **14**, 6089–6101 (2014).
60. Li, J. F. *et al.* Fast increasing of surface ozone concentrations in Pearl River Delta characterized by a regional air quality monitoring network during 2006–2011. *J Environ Sci-China* **26**, 23–36 (2014).
61. Pollack, I. B. *et al.* Trends in ozone, its precursors, and related secondary oxidation products in Los Angeles, California: A synthesis of measurements from 1960 to 2010. *J Geophys Res-Atmos* **118**, 5893–5911 (2013).
62. Zhang, Y. L. & Cao, F. Fine particulate matter (PM_{2.5}) in China at a city level. *Sci Rep-Uk* **5** (2015).
63. Stenfors, N. *et al.* Effect of ozone on bronchial mucosal inflammation in asthmatic and healthy subjects. *Resp Med* **96**, 352–358 (2002).
64. Vagaggini, B. *et al.* Ozone exposure increases eosinophilic airway response induced by previous allergen challenge. *Am J Resp Crit Care* **166**, 1073–1077 (2002).
65. Scannell, C. *et al.* Greater ozone-induced inflammatory responses in subjects with asthma. *Resp Med* **154**, 24–29 (1996).
66. Blomberg, A. *et al.* Clara cell protein as a biomarker for ozone-induced lung injury in humans. *Eur Respir J* **22**, 883–888 (2003).
67. U.S. EPA. *Guideline on data handling conventions for the 8-hour ozone NAAQS* Available at <https://nepis.epa.gov/Exe/ZyPDF.cgi/2000D5U0.PDF?Dockey=2000D5U0.PDF> (Accessed: 15 August 2016).
68. Mingxing, C., Yinghua, G., Yang, L., Dadao, L. & Hua, Z. Population distribution and urbanization on both sides of the Hu Huanyong Line: Answering the Premier's question. *J Geophys Res* **26**, 1593–1610 (2016).

Acknowledgements

This research was supported by National Natural Science Foundation of China (41371015, 41001207, 41401386, 41501401), and the Major Special Project-the China High-Resolution Earth Observation System (30-Y20A21-9003-15/17).

Author Contributions

T.-H.C. conceived and designed this study. W.-N.W. analyzed the data and wrote the manuscript. F.-W.B., S.-Y.S., and B.-R.X. draw the figures. X.Z., C.M. and X.-C.Z. prepared the database. X.-F.G., H.C., H.G. and Y.W. revised the paper critically.

Additional Information

Supplementary information accompanies this paper at doi:[10.1038/s41598-017-03929-w](https://doi.org/10.1038/s41598-017-03929-w)

Competing Interests: The authors declare that they have no competing interests.

Publisher's note: Springer Nature remains neutral with regard to jurisdictional claims in published maps and institutional affiliations.



Open Access This article is licensed under a Creative Commons Attribution 4.0 International License, which permits use, sharing, adaptation, distribution and reproduction in any medium or format, as long as you give appropriate credit to the original author(s) and the source, provide a link to the Creative Commons license, and indicate if changes were made. The images or other third party material in this article are included in the article's Creative Commons license, unless indicated otherwise in a credit line to the material. If material is not included in the article's Creative Commons license and your intended use is not permitted by statutory regulation or exceeds the permitted use, you will need to obtain permission directly from the copyright holder. To view a copy of this license, visit <http://creativecommons.org/licenses/by/4.0/>.

© The Author(s) 2017